



ELSEVIER

Journal of Alloys and Compounds 330–332 (2002) 831–834

Journal of
ALLOYS
AND COMPOUNDS

www.elsevier.com/locate/jallcom

Effects of particle size and heat treatment on the electrode performance of a low-cobalt atomized AB₅-type hydrogen storage alloy

Huang Yuexiang*, Ye Hui, Zhang Hong

Division of Energy Science and Technology, Shanghai Institute of Metallurgy, CAS, Shanghai 200050, PR China

Abstract

A low-cobalt hydrogen storage alloy with a composition of MLNi_{3.8}Co_{0.3}Fe_{0.2}Mn_{0.4}Al_{0.3} was prepared by a vacuum induction casting method followed by gas atomization processing. The results showed that the atomized powders had lower discharge capacity and poorer activation kinetics but better cycling stability than the as-cast sample. The high amount of oxygen and nitrogen present in the atomized powder and the presence of amorphous phase were the main reasons for the observed low discharge capacity and poor activation performance. The atomized powder with a large particle size showed a lower oxygen content and therefore higher discharge capacity than that with a small particle size. However the favorable effect of the atomization processing on the durability of the hydrogen storage alloy was eliminated after heat treatment at 850°C for 6 h. © 2002 Elsevier Science B.V. All rights reserved.

Keywords: Hydrogen storage materials; Atomization; Particle size; Heat treatment

1. Introduction

The nickel–metal hydride (Ni–MH) rechargeable battery, using a hydrogen storage alloy as its negative material, is a promising alternative to the conventional nickel–cadmium and lead–acid batteries because it is pollution-free and because of its superior performance, namely high energy density, long cycle life during electrochemical charge and discharge cycling, and good capability against overcharge and overdischarge [1]. It is generally recognized that the application performance of a Ni–MH battery is significantly influenced by the characteristics of the hydrogen storage alloy used. Gas atomization processing, as a rapid solidification technique, could provide considerable benefits in the production of hydrogen storage alloys over the conventional casting routes. Economically, it could reduce the material and processing costs during fabrication and, technically, it could produce a hydrogen storage alloy power with improved compositional homogeneity and fine-grained microstructure which are favorable for durability against corrosion in alkaline solution during electrochemical charge and discharge cycling.

Research on the application of gas atomized hydrogen storage alloys as an anode material in Ni–MH batteries has

been conducted by some authors [2–5]. Lichtenberg et al. [6] reported that gas atomized AB₅ type hydrogen storage alloys showed better electrode performance than alloys prepared by conventional casting processing, while the opposite has been observed by other authors [2–4]. In the later case the observed lower electrochemical capacity and poorer hydrogen absorption and desorption kinetics of gas atomized alloys compared to those of as-cast alloys were generally ascribed to severe oxidation during the atomization process or the presence of amorphous phases [3–5]. The different results observed for gas atomized alloys reflects the fact that a successful application of gas atomized alloys in Ni–MH batteries would largely depend on the control of oxidation during the fabrication process.

In the present work, a low-cobalt AB₅-type alloy with a composition of MLNi_{3.8}Co_{0.3}Fe_{0.2}Mn_{0.4}Al_{0.3} alloy (ML noted as lanthanum-rich mischmetal) was prepared by a gas atomization technique. The effects of alloy particle size and heat treatment on the electrode performance are reported.

2. Experimental procedure

The MLNi_{3.8}Co_{0.3}Fe_{0.2}Mn_{0.4}Al_{0.3} alloy ingot was prepared by vacuum inductive melting, using lanthanum-rich mischmetal, nickel, cobalt, manganese, aluminum and iron as raw materials. One portion of the obtained ingot was

*Corresponding author. Tel.: +86-21-6225-4273.

E-mail address: yuexiang@itsvr.sim.ac.cn (H. Yuexiang).

then ground into powder using a pestle and mortar and then sifted (noted as as-cast sample). The remaining ingot was atomized under high purity argon into powder (noted as atomized sample). The as-prepared powder was then classified into three portions by sieve. The annealing of the as-cast and atomized powders was carried out in a vacuum furnace by heating the powders to 850°C and holding for 6 h.

The particle size distribution of the various powders was measured by a Malvern particle size analyzer (Mastersizer 2000 model). D_{50} is defined as the particle size corresponding to 50% accumulation volume in the particle size distribution curve. X-ray diffraction spectra of various powders were obtained by an X-ray diffractometer (XRD; Philips, X'Pert MPD model), using Cu $K\alpha$ radiation. The morphology of the powder particles was observed by scanning electron microscopy (SEM; AMRAY 1000B model) using the secondary electron mode. The oxygen and nitrogen content in various powders was measured by an oxygen/nitrogen analyzer (LECO TC436 model).

The negative electrode pellets (15.5 mm in diameter) were prepared by mixing 0.3 g of alloy powder with 1.2 g of fine nickel powder, and then pressed on a piece of nickel mesh at 6 MPa for 1 min. The electrochemical measurements of these negative electrodes were performed in a half-cell with 6 M KOH solution at 20°C. A sintered nickel electrode with large capacity and a Hg/HgO 6 M KOH electrode were used as counter and reference electrodes respectively. The charge–discharge electric current was 60 mA/g and the cut-off potential for each discharging was set at -0.600 V versus Hg/HgO. The charging and discharging schedule for the cycle life measurement was as follows: charging at 300 mA/g for 1.2 h, resting 10 min and discharging at 300 mA/g until -0.600 V versus Hg/HgO.

3. Results and discussion

3.1. Powder characteristics

The observation of microstructure (not shown) shows that the particle morphology of the atomized powder is spherical and the as-cast sample is irregular. The XRD results (not shown) indicate that both the as-cast and atomized samples have a CaCu_5 -type crystal structure. Fig. 1 shows the particle size distribution curves of the three portions of the atomized and as-cast powders. The particle size distribution for the atomized powders is narrow. The average particle size of D_{50} is 265.5, 135.9 and 61.5 μm for the three portions of the atomized powders, and 62.5 μm for the as-cast sample.

3.2. Effect of particle size

Fig. 2 gives the activation curves of the electrodes prepared from the as-cast and atomized powders with

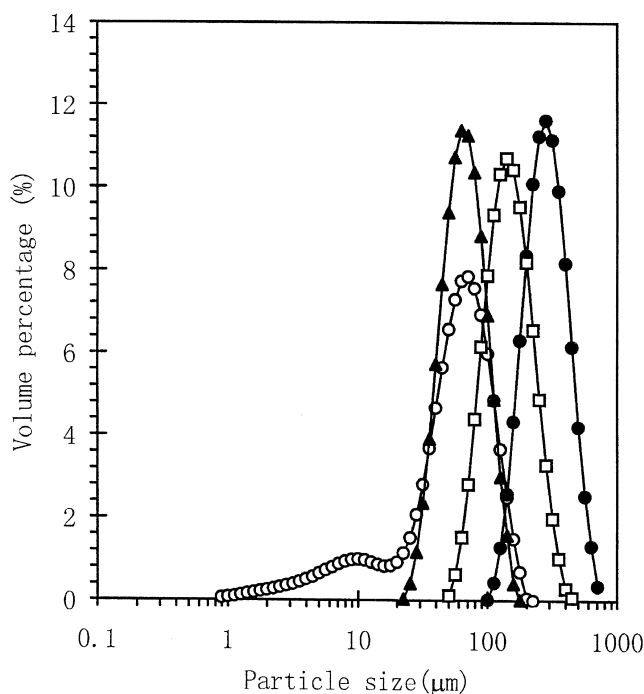


Fig. 1. Particle size distribution curves of various powders. (○), as-cast, $D_{50}=62.5$ μm ; (◻), atomized, $D_{50}=61.5$ μm ; (◻), atomized, $D_{50}=135.9$ μm ; (●), atomized, $D_{50}=265.5$ μm .

different particle size. It can be seen that the as-cast sample shows fast activation characteristic and after two charge and discharge cycles the maximum discharge capacity is obtained. For the atomized powders, the discharge capacity increases slowly, indicating the poor activation kinetics.

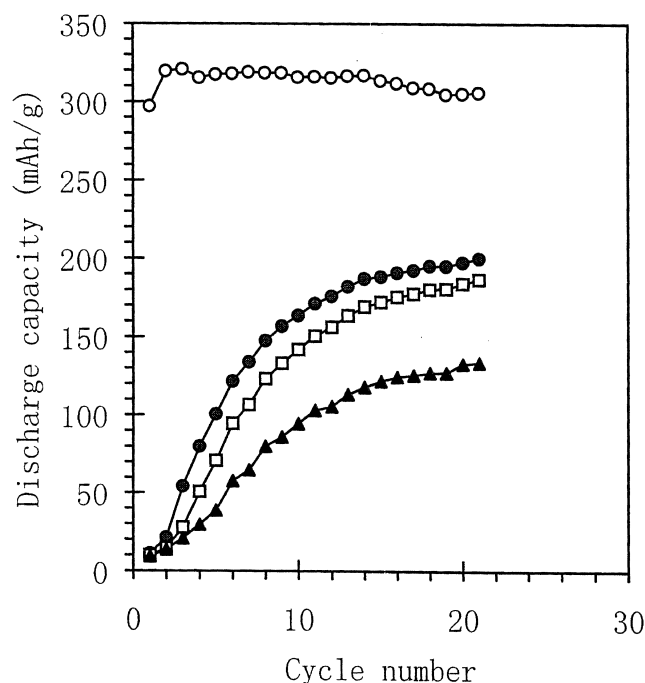


Fig. 2. Activation curves of various powders. (○), as-cast, $D_{50}=62.5$ μm ; (◻), atomized, $D_{50}=61.5$ μm ; (◻), atomized, $D_{50}=135.9$ μm ; (●), atomized, $D_{50}=265.5$ μm .

Similar behavior has also been observed by other researchers [2–4]. The maximum discharge capacity of the as-cast sample is 320 mAh/g and for the atomized powder it is in a range of 100–250 mAh/g, depending on the particle size. The larger the particle size, the higher the discharge capacity.

The contents of oxygen and nitrogen in the atomized and as-cast powders are listed in Table 1. It is observed that the oxygen and nitrogen contents are much higher in the atomized powders than in the as-cast powder, probably being taken up during the atomization process. This may be one of the most important reasons for the observed lower discharge capacity and poorer activation kinetics of the atomized powders compared to the as-cast sample. For the atomized powders, the larger the particle size, the lower the content of oxygen and the higher the discharge capacity, further verifying the detrimental effect of oxygen on the discharge capacity. However the effect of nitrogen content on the discharge capacity and activation kinetics seems minor for the atomized powders.

Fig. 3 shows the stability during charge and discharge cycling of the as-cast and atomized powders. It is seen that the atomized powders show better cycling stability than the as-cast sample. This is because the atomization processing can produce powders with better compositional homogeneity than those produced from conventional casting processing. For the atomized powder, the smaller the particle size, the better the cycling stability. This reflects the fact that the powder with a small particle size is obtained at a higher cooling rate than that with a large particle size. In other words, the observed difference in cycling stability of the atomized powders with different particle size is probably due to the different cooling rates attained.

The favorable effect of fine-grained microstructure, obtained by the rapid solidification processing methods, on the durability of hydrogen storage alloys has been observed. The smaller grain size and better compositional homogeneity of the atomized powders would increase the durability against corrosion in alkaline solution during electrochemical charge and discharge cycling. Furthermore, the high number of grain boundary phases present in the fine-grained atomized alloy might act as a ‘cushion’ and partially release the stresses occurring during the hydriding and dehydriding process. Therefore, the pulverization rate of the hydrogen storage alloys prepared by the rapid solidification techniques could be reduced and the cycling stability improved. It is probable that a combina-

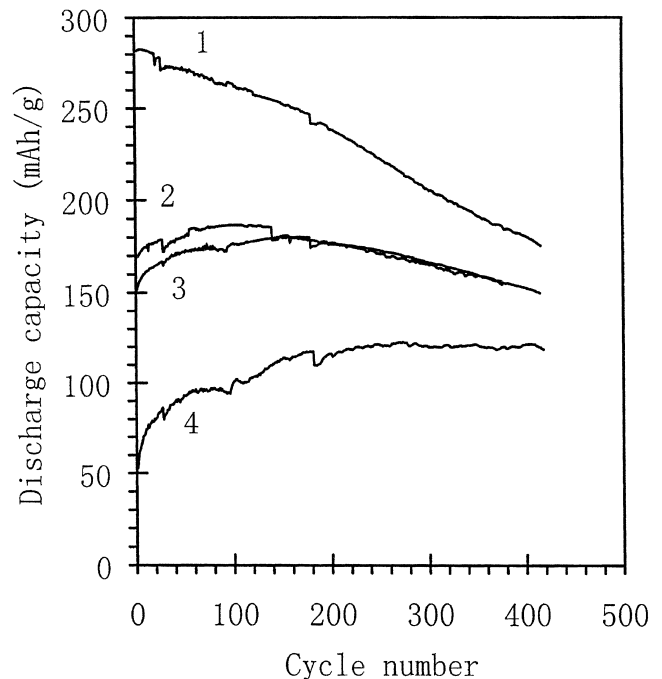


Fig. 3. Cycling stability of the electrodes prepared from various powders. (1), as-cast, $D_{50}=62.5 \mu\text{m}$; (2), atomized, $D_{50}=265.5 \mu\text{m}$; (3), atomized, $D_{50}=135.9 \mu\text{m}$; (4), atomized, $D_{50}=61.5 \mu\text{m}$.

tion of these effects contributes to the observed better durability of the atomized powders.

3.3. Effect of heat treatment

The as-cast and atomized powders with different particle size were annealed at 850°C for 6 h. The activation curves of the heat-treated samples are illustrated in Fig. 4. For the as-cast sample, the effect of heat treatment on the activation kinetics is minor, whereas the heat treatment can significantly improve the activation kinetics of the electrodes prepared from the atomized powders, though the oxygen content is slightly increased after heat treatment, as shown in Table 1. The discharge capacity of the atomized samples is also increased after heat treatment. As has been reported previously [5], some amorphous phase might be formed in the atomized powder as a consequence of the high solidification rate. When the sample is heated at a high temperature of 850°C, the crystallization of the amorphous phase may take place and therefore the activation kinetics would be improved and the discharge capacity increased. It is interesting to note that the effect of particle

Table 1
The measured contents of oxygen and nitrogen in various powders

Sample	As-cast powder, $D_{50}=62.5 \mu\text{m}$	Atomized powder, $D_{50}=265.5 \mu\text{m}$	Atomized powder, $D_{50}=135.9 \mu\text{m}$	Atomized powder, $D_{50}=61.5 \mu\text{m}$	Atomized powder, $D_{50}=61.5 \mu\text{m}$, (850°C/6 h)
Oxygen (ppm)	876	1893	2038	2378	2678
Nitrogen (ppm)	8	269	211	189	188

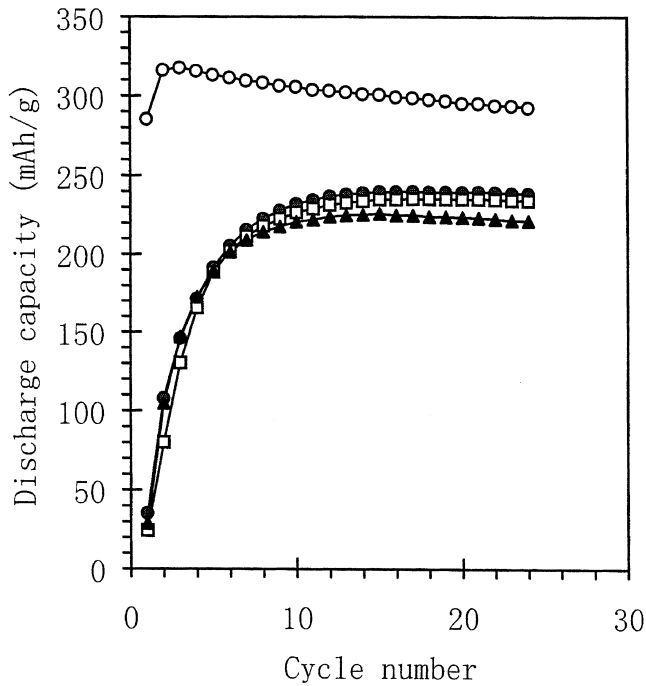


Fig. 4. Activation curves of various powders after heat treatment at 850°C for 6 h. (O), as-cast, $D_{50}=62.5 \mu\text{m}$; (•), atomized, $D_{50}=61.5 \mu\text{m}$; (◻), atomized, $D_{50}=135.9 \mu\text{m}$; (●), atomized, $D_{50}=265.5 \mu\text{m}$.

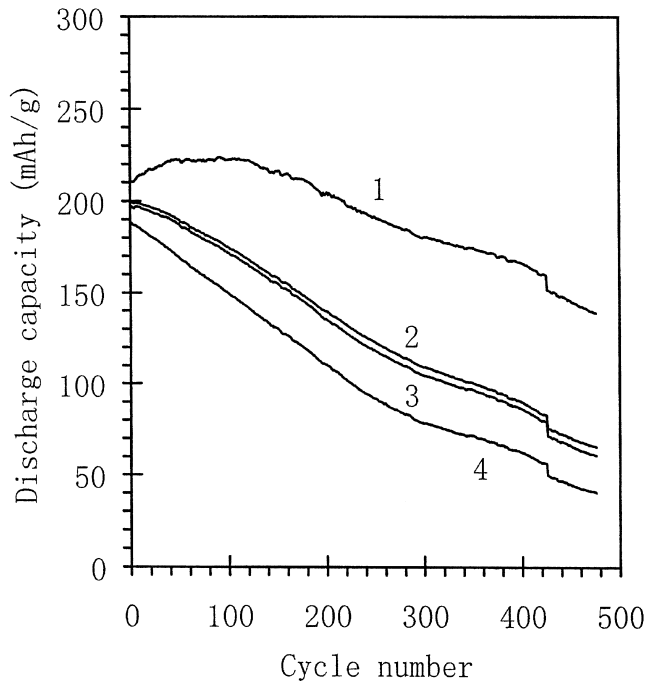


Fig. 5. Cycling stability of the electrodes prepared from various powders after heat treatment at 850°C for 6 h. (1), as-cast, $D_{50}=62.5 \mu\text{m}$; (2), atomized, $D_{50}=265.5 \mu\text{m}$; (3), atomized, $D_{50}=135.9 \mu\text{m}$; (4), atomized, $D_{50}=61.5 \mu\text{m}$.

size on the activation kinetics and maximum discharge capacity becomes less important after heat treatment.

Fig. 5 shows the cycling stability of various samples after heat treatment at 850°C for 6 h. It is evident that the favorable effect on the cycling stability, caused by the rapid solidification, is eliminated after heat treatment.

4. Conclusions

The poor cycling stability of the low-cobalt $\text{MLNi}_{3.8}\text{Co}_{0.3}\text{Fe}_{0.2}\text{Mn}_{0.4}\text{Al}_{0.3}$ hydrogen storage alloy was improved by atomization processing, though the discharge capacity and activation kinetics simultaneously deteriorated, which was ascribed to the high amount of oxygen and nitrogen present in the atomized powders and the presence of amorphous phase. For the atomized powder, the larger the particle size, the lower the oxygen content and the better the discharge capacity and activation kinetics. The effect of nitrogen content on the discharge capacity and activation kinetics seemed minor. The improved durability of the hydrogen storage alloy, obtained by the atomization processing, was eliminated after heat treatment at 850°C for 6 h.

Acknowledgements

The first author gratefully acknowledges the support of K.C. Wong Education Foundation, Hong Kong.

References

- [1] C. Iwakura, M. Matsuoka, Prog. Batteries Battery Mater. 10 (1991) 81–114.
- [2] Yu.M. Solonin, V.V. Savin, S.M. Solonin, V.V. Skorokhod, L.L. Kolomiets, T.I. Bratanich, J. Alloys Comp. 253–254 (1997) 594–597.
- [3] R.C. Bowman Jr., C. Witham, B. Fultz, B.V. Ratnakumar, T.W. Ellis, I.E. Anderson, J. Alloys Comp. 253–254 (1997) 613–616.
- [4] H.S. Lim, G.R. Zelter, D.U. Allison, R.E. Haun, J. Power Sources 66 (1997) 101–105.
- [5] H. Yuexiang, Z. Hong, J. Alloys Comp. 305 (2000) 76–81.
- [6] F. Lichtenberg, U. Kohler, F. Folzer, N.J.E. Adkins, A. Zuttel, J. Alloys Comp. 253–254 (1997) 570–573.